LETTERS

Acceleration of neutral atoms in strong short-pulse laser fields

U. Eichmann[1,2], T. Nubbemeyer[1], H. Rottke[1] & W. Sandner[1,2]

A charged particle exposed to an oscillating electric field experiences a force proportional to the cycle-averaged intensity gradient. This so-called ponderomotive force[1] plays a major part in a variety of physical situations such as Paul traps[2,3] for charged particles, electron diffraction in strong (standing) laser fields[4–6] (the Kapitza–Dirac effect) and laser-based particle acceleration[7–9]. Comparably weak forces on neutral atoms in inhomogeneous light fields may arise from the dynamical polarization of an atom[10–12]; these are physically similar to the cycle-averaged forces. Here we observe previously unconsidered extremely strong kinematic forces on neutral atoms in short-pulse laser fields. We identify the ponderomotive force on electrons as the driving mechanism, leading to ultrastrong acceleration of neutral atoms with a magnitude as high as $\sim 10^{14}$ times the Earth's gravitational acceleration, *g*. To our knowledge, this is by far the highest observed acceleration on neutral atoms in external fields and may lead to new applications in both fundamental and applied physics.

The investigation has become possible through two recent findings concerning atomic ionization dynamics in strong laser fields. First, neutral atoms can survive a strong laser field in a (long-lived) excited state[13], in which they can be detected directly in an atomic beam by means of a standard electron or ion detector[14]. Thus, any momentum transferred to the neutral atom can easily be detected. Second, according to the physical picture behind the excitation process, the excited electron behaves as a quasi-free electron during the laser pulse. More precisely, the excitation process can be viewed as a frustrated tunnel ionization[14] within the three-step model for strong-field ionization[15].

In the first step, the electron tunnels in the close vicinity of the maximum electric field of a laser cycle. The liberated electron is then driven by the laser field with an amplitude that slowly decreases with decreasing pulse intensity; in this way an active damping of the electronic motion takes place. After the laser pulse the electron is left with a drift energy too low to overcome the Coulomb potential of the ion and is recaptured into a Rydberg state. The quivering quasi-free electron experiences the ponderomotive force during the laser pulse owing to the intensity gradient in the focused laser beam. We will show here that the quiver motion of the electron is partially converted into centre-of-mass motion of the neutral atom, leading to a substantial acceleration. This results in a measurable momentum transfer to the atom despite the short interaction time in the femtosecond range. Remarkably, the ponderomotive effect is typically estimated to be negligible for these conditions[16,17] with, however, a few exceptions[18]. We note that the investigation relies on the highly selective process of excitation of neutrals in a strong laser field, where kinematic effects are imparted only through the gradient of the laser field.

In the experiment we excite neutral He atoms in an effusive atomic beam using a perpendicularly intersecting focused laser beam. Using the detection technique (see the Methods) we measure the distribution of excited He atoms on a detector as shown in Fig. 1. If, during the laser pulse, no momentum is transferred to the atoms, we would expect a slightly enlarged projected image of the (laser-intensity-dependent) distribution of excited atoms in the laser beam on the detector, that is, a distribution that extends along the laser beam direction (z axis), typically within the Rayleigh length, but with a very narrow radial distribution (r_D axis) of the order of the size of the laser beam waist.

In Fig. 1a, however, we see a strikingly large radial distribution of excited atoms with a strong maximum in the laser focal plane ($z = 0$) that obviously stems from a deflecting radial force during the laser pulse. In Fig. 1b the cut along the z axis (black curve) shows two maxima at roughly half the laser peak intensity $I_0/2$, where the net production rate of excited helium atoms He* is apparently maximum, whereas the He* signal at I_0 shows a pronounced minimum. However, the loss of neutral excited atoms is largely due to their radial deflection. The full projection (red dashed curve) shows only a slight decrease in signal, indicating that even at the highest intensities He atoms are excited. The data are taken at a low beam target pressure of $\simeq 5 \times 10^{-7}$ mbar. The radial deflection is unchanged when we increase the target pressure by more than a factor of 30. This excludes many-particle effects based on atom density or space charge as an origin of our observations. Furthermore, we emphasize that the radial distribution is unaltered whether the linear polarization of the laser beam is in the direction of the atomic beam or perpendicular to it. In this respect the intensity-dependent force very much resembles the ponderomotive force acting on charged particles. The question arises whether we can conclude that the ponderomotive force is responsible for the observed centre-of-mass motion of the neutral particle.

To shed light on the underlying process we first recall that the ponderomotive force $\mathbf{F}_p$ on a charged particle is given by (all equations are in atomic units):

$$\mathbf{F}_p = -\frac{q^2}{4m\omega^2}\nabla|\mathbf{E}_0|^2 \qquad (1)$$

Here, m and q are the mass and the charge of the particle, respectively, $\mathbf{E}(\mathbf{r}, t) = \mathbf{E}_0(\mathbf{r}, t)\exp i\omega t$ is the electric field, ω is the field frequency and $\mathbf{E}_0(\mathbf{r}, t)$ is the slowly varying field amplitude. Hence, in view of our frustrated tunnel ionization model, both the ionic core and the electron experience a mass-dependent ponderomotive force during the laser pulse. As a consequence of the mass dependency, however, the ionic core remains practically unaffected while the electron experiences a non-negligible ponderomotive force. This, in turn, means that to the first approximation a ponderomotive force acts directly on the centre-of-mass motion of the atom and leaves the recapturing process unaffected. This can be shown more rigorously: we derive the centre-of-mass motion from the Lorentz force (see the

[1]Max-Born-Institute, Max-Born-Strasse 2a, 12489 Berlin, Germany. [2]Institut für Optik und Atomare Physik, Technische Universität Berlin, 10632 Berlin, Germany.

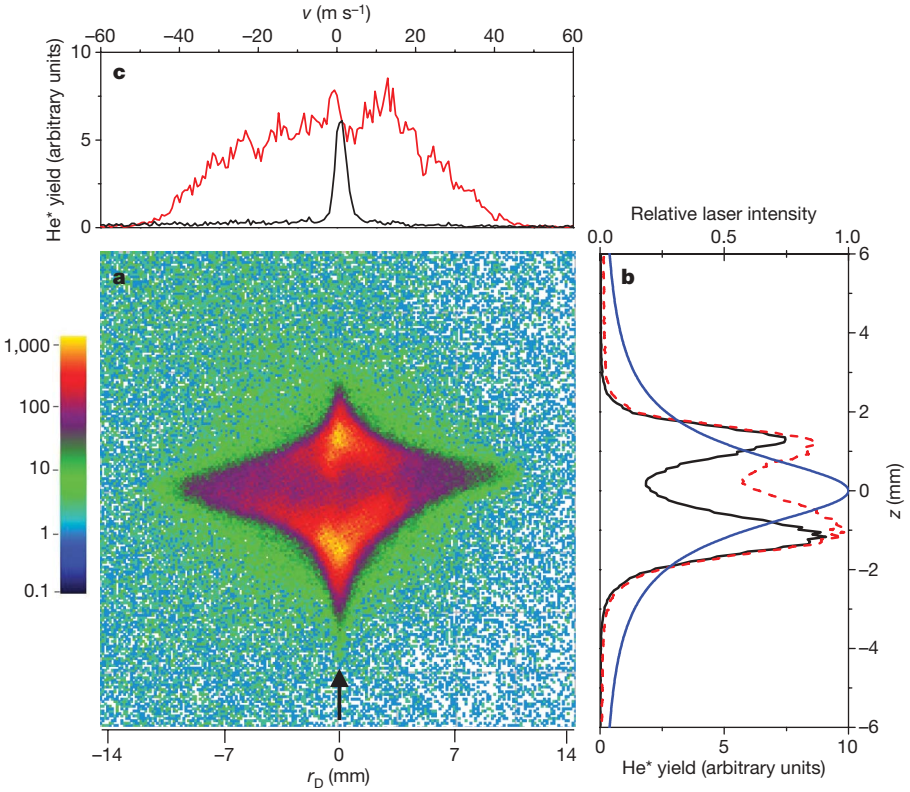

Figure 1 | Deflection of neutral He atoms after interaction with a focused laser beam. a, Distribution of excited He* atoms on the detector (colour scale, in number of atoms). The laser beam direction is indicated by the arrow. **b**, Cut through the atom distribution along the laser beam axis (z axis) at $r_D = 0$ mm (black curve) and full projection on z axis (dashed red curve) and intensity along the z axis in units of the laser peak intensity $I_0 = 6.9 \times 10^{15}$ W cm^{-2} (blue curve). **c**, Cuts through the distribution at $z = 0$ mm (red curve) and $z = -2.7$ mm (black curve). The black curve shows the velocity distribution of excited neutral atoms at a position unaffected by the ponderomotive force, showing essentially the 'natural' velocity spread, while the red curve shows the velocity gain through the ponderomotive force.

online-only Methods). Recalling the key point of our investigation, that the electron remains bound after interaction with the laser pulse, we are able to observe the centre-of-mass motion. Furthermore, by solving the coupled Lorentz equations for the electron and the ion, including the Coulomb potential, we can directly reproduce the capture process into bound Rydberg orbits and the force on the centre of mass.

According to our model we can rewrite equation (1) for the centre-of-mass position $\mathbf{R}$ of the neutral atom:

$$M\ddot{\mathbf{R}}(t) = -\frac{1}{4m_e\omega^2}\nabla|\mathbf{E}_0|^2 \qquad (2)$$

Here, M and m_e (= 1 atomic unit) are the masses of the atom and the electron, respectively, and $\ddot{\mathbf{R}}(t)$ is the second derivative of the centre-of-mass position $\mathbf{R}$ with respect to time. To calculate the ponderomotive force explicitly, we assume a linearly polarized laser beam with a Gaussian spatial intensity distribution, which reads, in cylindrical coordinates:

$$I(\mathbf{r}) = |\mathbf{E}_0(\mathbf{r})|^2 = I_0\left(1+\left(\frac{z}{z_0}\right)^2\right)^{-1}\exp\frac{-2r^2}{r_0^2} \qquad (3)$$

where $r_0 = w_0\sqrt{1+(z/z_0)^2}$, w_0 is the beam waist. Evaluating the gradient in equation (2) with the intensity distribution given by equation (3), we obtain, for the radial component of the centre-of-mass position perpendicular to the laser beam direction:

$$\ddot{r}(t) = \frac{I(\mathbf{R})}{M\omega^2}\frac{r(t)}{r_0^2}f(t) \qquad (4)$$

where $f(t)$ is the laser pulse envelope, which we assume to be of the form $f(t) = \exp(-t^2/\tau^2)$, where τ is the pulse width. From equation (4) we find that the maximum force along the radial direction scales as r_0^{-1}. Similarly, one can show that it scales as z_0^{-1} along the laser beam direction. Because the Rayleigh length z_0 is typically a factor of 100 larger than the beam waist r_0, the gradient and thus the ponderomotive force in the laser beam direction is much smaller than in the radial direction and can be neglected. (However, the situation would be very different if we used a short-pulse standing-wave laser field. We would then obtain a strong periodic intensity gradient on the scale of the laser wavelength, and might expect to see the Kapitza–Dirac effect for neutral atoms in an intense standing-wave laser field instead of electrons[19]).

To solve equation (4), we assume that the neutral atom does not move significantly during the laser pulse. Hence, we set $r(t) = r$ on the right-hand side of the equation, which allows us to solve equation (4) analytically for any initial position of an atom in the laser beam. We will concentrate our analysis on atoms located at the half beam size $r_0/2$, which experience the maximum force. Solving equation (4) for these conditions by integrating over the full laser pulse, we find the maximum velocity $v_{max}(z)$:

$$v_{max}(z) = \frac{I_0}{2M\omega^2 w_0}\frac{\sqrt{\pi}\exp(-0.5)}{\sqrt{1+\left(\frac{z}{z_0}\right)^2}}\tau \qquad (5)$$

If we evaluate equation (5) at the focal plane for He atoms exposed to our focused laser beam at maximum intensity, we obtain a velocity of about 55 m s^{-1} from which accelerations of about $2 \times 10^{14} g$ can be deduced.

This exceeds the typical acceleration (deceleration) of neutral atoms[20] or molecules in external fields[21,22]. Compared to laser-cooling experiments in a continuous-wave laser field, for instance, which are

based on photon momentum transfer with a typical deceleration of about $10^6 g$ (ref. 20), the acceleration present in our experiment is eight orders of magnitude larger. It is, to the best of our knowledge, by far the largest acceleration of neutral matter by electromagnetic fields ever observed.

Finally, we mention that a different but equivalent description of our process might be given in terms of an atom in the Kramers–Henneberger reference frame[23], which is expected to exhibit stable configurations in a strong electromagnetic field. Our observations of accelerated neutral atoms seem to be a direct confirmation of the existence of this exotic type of stable atom.

In Fig. 2 we show the results of a systematic investigation of He atoms exposed to laser light of different laser pulse lengths and laser pulse energy E_L, such that the laser intensity is kept constant. We obtain neutral excited atom distributions similar to the one shown in Fig. 1. The maximum radial deflection of the atoms along the laser beam axis, which can be converted into maximum velocity $v_{max}(z)$, can reliably be extracted from the experimental data to compare with equation (5). Fitting equation (5) to the data gives very good agreement, confirming the validity of our model. The fit contains only three free parameters: a small velocity offset, a common constant beam waist w_0, and a scaling factor for the absolute velocity. The best choice of the latter implies that the acceleration must last over the whole pulse duration, confirming the assumption that the electrons are set free early during the laser pulse.

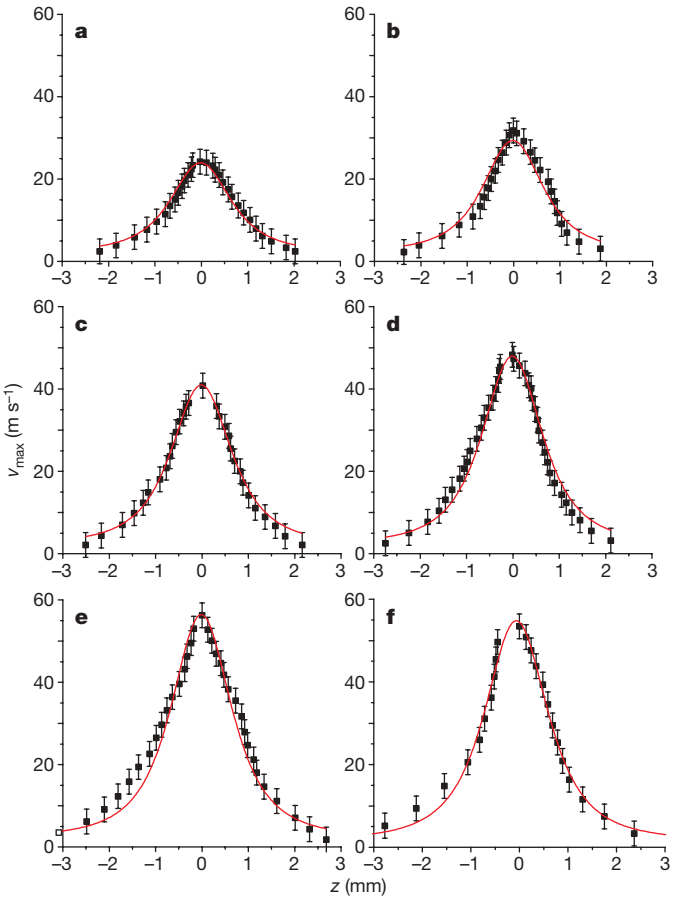

Figure 2 | Maximum velocity $v_{max}(z)$ gained by neutral He atoms. **a**–**e**, $v_{max}(z)$ extracted from measurements at constant laser peak intensity $I_0 = 2.8 \times 10^{15}$ W cm^{-2} (3.4×10^{15} W cm^{-2}), but for different pulse energies E_L and pulse durations τ_{FWHM}: **a**, 600 μJ, 40 fs; **b**, 900 μJ, 60 fs; **c**, 1.2 mJ, 80 fs; **d**, 1.5 mJ, 100 fs; **e**, 1.8 mJ, 120 fs. FWHM, full-width at half-maximum. The red curves are fits to the data based on equation (5). The fitted common beam waist $w_0 = 16.0$ μm is in good agreement with an independent experimental determination of $w_0 = 17.5 \pm 1.5$ μm using the knife-edge method. It results, however, in a higher laser peak intensity, which is indicated in parentheses. **f**, $v_{max}(z)$ for laser parameters $E_L = 1.8$ mJ and $\tau_{FWHM} = 40$ fs corresponding to $I_0 = 8.3 \times 10^{15}$ W cm^{-2} (10×10^{15} W cm^{-2}). The error bars are estimated from the accuracy of the maximum deflection we determined.

Even then the observed velocities lie slightly above the theoretical prediction (see Fig. 3), which we attribute to absolute laser intensity uncertainties or a slightly non-Gaussian intensity distribution. Hence, we note that the radial velocity $v_{max}(z)$ might serve as a valuable beam shape and intensity parameter along the laser beam axis. On the one hand it measures the peak intensity if the radial intensity distribution is known (for example, Gaussian), or, on the other hand, indicates systematic deviations from the Gaussian beam shape if the peak intensity is known (for example, from ionization experiments). Such information is otherwise rather difficult to obtain.

We have also measured the radial deflection of a beam of Ne atoms, which is, however, smaller than in He, as expected owing to the larger mass. In Fig. 3 we show the maximum velocity $v_{max}(z = 0)$ transferred to Ne atoms exposed to a laser beam kept at a constant laser intensity of $I_0 = 2.8 \times 10^{15}$ W cm^{-2}, but at different pulse durations and energies. For comparison, the maximum velocities for He are also shown. The data clearly show the excellent quantitative agreement of the observed deflection with our theoretical predictions. Within the range of our achievable pulse durations the deflection is proportional to the mass and the time the force is acting on the atom.

In conclusion, we have demonstrated ultrastrong acceleration of neutral atoms, using femtosecond laser pulses with intensities of up to $I_0 = 10^{16}$ W cm^{-2}. We present a quantitative theoretical model based on the concept that a bound electron temporarily undergoes a quasi-free oscillatory quiver motion during the laser pulse while still being coupled to the ion by the Coulomb force. The inhomogeneous field of a focused laser beam causes a ponderomotive force on the electron, resulting in a centre-of-mass acceleration of the whole atom. Many new applications may be envisioned, considering that the mechanism transfers the momenta of a large number (presently of the order of 10^3) of photons quasi-instantaneously onto neutral atoms, without any problems due to Doppler detuning, as in the case of resonant continuous-wave laser absorption. Atom optics, controlled atom deposition or controlled chemical reactions are just some of them. The acceleration process may be considerably refined by sophisticated spectral and temporal shaping of the accelerating laser beam, including the use of standing (or slowly moving) waves with much steeper field gradients, or the use of longer pulse durations for achieving substantially larger atomic momenta.

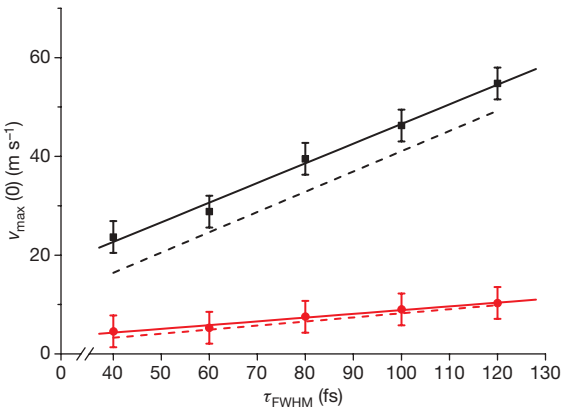

Figure 3 | Maximum velocity $v_{max}(0)$ transferred to He and Ne at the focal plane as a function of the laser pulse duration at constant laser intensity. $v_{max}(0)$ is plotted for He (black squares) and Ne (red circles) measured at $I_0 = 2.8 \times 10^{15}$ W cm^{-2} (3.4×10^{15} W cm^{-2}); see explanation in Fig. 2. The dashed black and red curves show the calculated velocities, respectively, using equation (5) with the fitted beam waist, but omitting the scaling factor. The full curves are fits to the data. The error bars are determined as in Fig. 2.

METHODS SUMMARY

The observation of acceleration of neutral atoms in strong laser fields is based on the method of producing and detecting excited neutral atoms in strong laser fields introduced in ref. 14. In the online-only Methods we give a detailed description of how to adapt the method to the present experiments. Furthermore, we detail the theoretical background of the underlying process and derive the respective formulas used to describe our data.

Full Methods and any associated references are available in the online version of the paper at www.nature.com/nature.

Received 15 May; accepted 27 August 2009.

1. Kibble, T. W. B. Refraction of electron beams by intense electromagnetic waves. *Phys. Rev. Lett.* **16,** 1054–1056 (1966).
2. Boot, H. A. H., &. Harvie, R. B. R.-S. Charged particles in a non-uniform radio-frequency field. *Nature* **180,** 1187 (1957).
3. Dehmelt, H. G. Radio-frequency spectroscopy of stored ions. *Adv. At. Mol. Phys.* **3,** 53–72 (1967).
4. Kapitza, P. & Dirac, P. The reflection of electrons from standing light waves. *Proc. Camb. Philos. Soc.* **29,** 297–300 (1933).
5. Bucksbaum, P. H., Schumacher, D. W. & Bashkansky, M. High-intensity Kapitza-Dirac effect. *Phys. Rev. Lett.* **61,** 1182–1185 (1988).
6. Freimund, D. L., Aflatooni, K. & Batelaan, H. Observation of the Kapitza-Dirac effect. *Nature* **413,** 142–143 (2001).
7. Tajima, T. & Dawson, J. M. Laser electron accelerator. *Phys. Rev. Lett.* **43,** 267–270 (1979).
8. Geddes, C. *et al.* High-quality electron beams from a laser wakefield accelerator using plasma-channel guiding. *Nature* **431,** 538–541 (2004).
9. Mourou, G., Tajima, T. & Bulanov, S. Optics in the relativistic regime. *Rev. Mod. Phys.* **78,** 309–371 (2006).
10. Gould, P. L., Ruff, G. A. & Pritchard, D. E. Diffraction of atoms by light: The near-resonant Kapitza-Dirac effect. *Phys. Rev. Lett.* **56,** 827–830 (1986).
11. Chu, S., Bjorkholm, J. E., Ashkin, A. & Cable, A. Experimental observation of optically trapped atoms. *Phys. Rev. Lett.* **57,** 314–317 (1986).
12. Grimm, R., Weidemüller, M. & Ovchinnikov, Y. Optical dipole traps for neutral atoms. *Adv. At. Mol. Phys.* **42,** 95–170 (2000).
13. de Boer, M. P. & Muller, H. G. Observation of large populations in excited states after short-pulse multiphoton ionization. *Phys. Rev. Lett.* **68,** 2747–2750 (1992).
14. Nubbemeyer, T., Gorling, K., Saenz, A., Eichmann, U. & Sandner, W. Strong-field tunneling without ionization. *Phys. Rev. Lett.* **101,** 233001 (2008).
15. Corkum, P. B. Plasma perspective on strong field multiphoton ionization. *Phys. Rev. Lett.* **71,** 1994–1997 (1993).
16. Krapchev, V. B. Kinetic theory of the ponderomotive effects in a plasma. *Phys. Rev. Lett.* **42,** 497–500 (1979).
17. McNaught, S. J., Knauer, J. P. & Meyerhofer, D. D. Photoelectron initial conditions for tunneling ionization in a linearly polarized laser. *Phys. Rev. A* **58,** 1399–1411 (1998).
18. Wells, E., Ben-Itzhak, I. & Jones, R. R. Ionization of atoms by the spatial gradient of the pondermotive potential in a focused laser beam. *Phys. Rev. Lett.* **93,** 023001 (2004).
19. Batelaan, H. Illuminating the Kapitza-Dirac effect with electron matter optics. *Rev. Mod. Phys.* **79,** 929–941 (2007).
20. Chu, S. Nobel lecture: The manipulation of neutral particles. *Rev. Mod. Phys.* **70,** 685–706 (1998).
21. Stapelfeldt, H., Sakai, H., Constant, E. & Corkum, P. B. Deflection of neutral molecules using the nonresonant dipole force. *Phys. Rev. Lett.* **79,** 2787–2790 (1997).
22. Fulton, R., Bishop, A. I. & Barker, P. F. Optical Stark decelerator for molecules. *Phys. Rev. Lett.* **93,** 243004 (2004).
23. Henneberger, W. C. Perturbation method for atoms in intense light beams. *Phys. Rev. Lett.* **21,** 838–841 (1968).

Acknowledgements We thank F. Noack for technical support on the laser system and W. Becker, P. B. Corkum, H. R. Reiss and O. Smirnova for discussions.

Author Contributions U.E. and T.N. designed and performed the experiments and analysed the data. All authors contributed to the theoretical understanding and were involved in the completion of the manuscript.

Author Information Reprints and permissions information is available at www.nature.com/reprints. Correspondence and requests for materials should be addressed to U.E. (ulli.eichmann@mbi-berlin.de).

METHODS

Experimental set-up and detection of excited neutral atoms. We use a slightly modified version of an experimental set-up that has been described elsewhere[14]. Briefly, a linearly polarized Ti:sapphire laser beam with a repetition rate of 500–1,000 Hz, a variable pulse width of $\tau_{FWHM} = 40$–120 fs and pulse energies up to 2.5 mJ is steered into a vacuum chamber with a base pressure of $\sim 10^{-9}$ mbar. It is focused by means of a plano-convex lens with a focal length of 0.2 m into an effusive beam of He or Ne atoms at right angles, where, among other processes, it excites neutral atoms. The beam target pressure is typically $\leq 5 \times 10^{-7}$ mbar. 0.38 m downstream in the direction of the atomic beam, a position-sensitive microchannel plate detector is located. The detector can be configured to detect either ions or electrons in the counting mode. Both configurations are suitable for excited neutral species detection, if they have an excitation energy of more than ~5 eV. In contrast to charged particles, which are easily accelerated by small electric fields (either deliberately applied or stemming from spurious charges) and hit the detector after a few microseconds, neutral atoms travel at thermal velocities reaching the detector only after hundreds of microseconds. Consequently, the excited state needs to survive long enough that the atom can reach the detector in an excited state. It has been found in earlier work[14] that an intense laser interacting with a beam of rare gas atoms produces mainly Rydberg states with principal quantum numbers around $n = 10$, which decay partially to a metastable state with high excitation energy, for example, ~20 eV in He. The metastable state lives long enough to reach the detector. We estimate that about 1% of all excited atoms reach the detector in an excited state.

Owing to the divergence of the atomic beam, the signal on the detector in laser beam direction is an image enlarged by a factor of 2.3 of the distribution of excited atoms in the laser beam, in case the momentum transferred to the atom during the excitation can be neglected. This needs to be taken into account when transforming the detector signal along the z_D coordinate into the laser beam z coordinate. The high detection sensitivity to accelerating forces during the laser pulse lies in the nature of neutral excited atoms travelling with thermal velocities. The time-of-flight distribution of He atoms at the microchannel plate detector peaks around 230 μs. Because momentum is only transferred to the atoms during the laser pulse duration, the starting point of the atoms is well defined. By setting a 40-μs-wide gate on the maximum of the time-of-flight distribution, a precise determination of the radial velocity can be calculated from the radial beam deflection on the detector. We note that the centre-of-mass motion of a neutral atom is largely unaffected by spurious electric fields or space charge.

Derivation of the ponderomotive centre-of-mass force on neutral atoms. To derive the centre-of-mass force on the neutral atom we solve the coupled Lorentz equations for the ion with mass m_1 and charge q_1 and electron with mass m_2 and charge q_2 including the Coulomb interaction between them. The two Lorentz equations in atomic units read:

$$\mathbf{F}_1 = m_1\ddot{\mathbf{r}}_1 = q_1(\mathbf{E}_1 + \mathbf{v}_1 \times \mathbf{B}_1) + \mathbf{F}_c \tag{6}$$

$$\mathbf{F}_2 = m_2\ddot{\mathbf{r}}_2 = q_2(\mathbf{E}_2 + \mathbf{v}_2 \times \mathbf{B}_2) - \mathbf{F}_c \tag{7}$$

where $\mathbf{E}_i \equiv \mathbf{E}(\mathbf{r}_i, t)$ and $\mathbf{B}_i \equiv \mathbf{B}(\mathbf{r}_i, t)$. The Coulomb force $\mathbf{F}_c$ is given by $\mathbf{F}_c = q_1 q_2 \frac{(\mathbf{r}_1 - \mathbf{r}_2)}{|\mathbf{r}_1 - \mathbf{r}_2|^3}$. Using the first-order electric and magnetic fields for a focused Gaussian beam[24], we can write the equations explicitly:

$$\begin{aligned} m_1\ddot{x}_1 &= E_{1x} + \dot{y}_1 B_{1z} - \dot{z}_1 B_{1y} + F_{cx} \\ m_1\ddot{y}_1 &= -\dot{x}_1 B_{1z} + F_{cy} \\ m_1\ddot{z}_1 &= \dot{x}_1 B_{1y} + F_{cz} + E_{1z} \end{aligned} \tag{8}$$

$$\begin{aligned} m_2\ddot{x}_2 &= -E_{2x} - \dot{y}_2 B_{2z} + \dot{z}_2 B_{2y} - F_{cx} \\ m_2\ddot{y}_2 &= \dot{x}_2 B_{2z} - F_{cy} \\ m_2\ddot{z}_2 &= -\dot{x}_2 B_{2y} - F_{cz} - E_{2z} \end{aligned} \tag{9}$$

Equation (2) can be derived analytically from the Lorentz forces using centre-of-mass and relative coordinates. We obtain the force on the centre-of-mass by using the following approximations. The fields are approximated to first order and we assume the slowly varying amplitude approximation; the relative velocity and position are approximated through the motion of the electron in the electric field in polarization (x) direction, neglecting the Coulomb force.

By solving equations (8) and (9) numerically without the aforementioned approximations, we obtain, for specific initial conditions, the bound trajectories of the tunnel electron at the end of the laser pulse as described in ref. 14. Most importantly, by evaluating the centre-of-mass velocity from the numerical calculations we confirm the results of equation (2).

To give an interpretation of why the electron remains bound, we first note that its motion during the laser pulse is mainly driven by the laser field. If we suppose that the electron starts at a maximum of a field cycle close to the nucleus, that is, where the Coulomb field is strong, the electron then revisits its starting (inner turning) point periodically with the laser frequency. Here, the attractive force is strongly peaked. For example, if the electron is set free at a distance of 10 atomic units (a.u.) from the nucleus, the Coulomb force is 10^{-2} a.u. acting for roughly a tenth of the laser cycle duration. If one compares this periodical force with the steady ponderomotive force $\mathbf{F}_p$, which is of the order of 10^{-4} a.u. for $I = 0.1$ a.u. and beam waist of $w_0 = 16$ μm we find an attractive net force.

Sign of the centre-of-mass force on a neutral atom in a laser field. A focus of a continuous-wave laser beam can act as a quasi-static dipole trap for neutral atoms[12] provided the photon energy of the laser is much below the lowest excited state. In this case the atom is a strong-field seeker. In our experiment, the force on the centre-of-mass motion according to equation (4) is outward bound, that is, the atom in the strong short-pulsed laser field is a low-field seeker, although the photon energy of the laser field is much below the lowest excited state. Obviously, the effective polarizability of an atom in a strong laser field, where the electron can be treated as quasi-free, differs in sign from a ground-state atom in a weak continuous laser field, where the strongly bound electron is only weakly perturbed by the laser field. According to the analysis of ref. 25 there is a relationship between the dynamical polarizability of an atom and the ponderomotive potential for a free electron U_p, from which the ponderomotive force can be obtained by $F_p = -\nabla U_p$. For a quasi-free electron, as is the case for our experiments, $U_p = \frac{e^2}{4m\omega^2} E^2$. The more general ponderomotive potential for a bound electron with a binding frequency ω_b is given by $U_p = \frac{e^2}{4m\left(\omega^2 - \omega_b^2\right)} E^2$, which can be derived from the Lorentz model of atomic polarizability. It is immediately obvious that for a strongly bound electron with $\omega \ll \omega_b$ the sign of the ponderomotive potential is opposite and the absolute value is much smaller than for a free electron.

24. Quesnel, B. & Mora, P. Theory and simulation of the interaction of ultraintense laser pulses with electrons in vacuum. *Phys. Rev. E* **58**, 3719–3732 (1998).
25. Eberly, J. H., Javanainen, J. & Rzazewski, K. Above-threshold ionization. *Phys. Rep.* **204**, 331–383 (1991).